Spring 5-3-2011

Experiments and Modelling of Micro-Jet Assisted Fluidization of Nanopowder

Ruud van Ommen
Delft University of Technology, j.r.vanommen@tudelft.nl

David M. King
University of Colorado Boulder, david.m.king@colorado.edu

Alan Weimer
University of Colorado Boulder, alan.weimer@colorado.edu

Robert Pfeffer
Arizona State University, robert.pfeffer@asu.edu

Berend van Wachem
Imperial College London, b.van-wachem@imperial.ac.uk

See next page for additional authors

EXPERIMENTS AND MODELLING OF MICRO-JET ASSISTED FLUIDIZATION OF NANOPOWDER

J. Ruud van Ommen[1], David M. King[2], Samantha Johnson[2], Niels Looije[1], Alan W. Weimer[2], Robert Pfeffer[3], Berend G.M. van Wachem[4]

[1]Department of Chemical Engineering, Delft University of Technology
Julianalaan 136, 2628 BL Delft, The Netherlands
T: +3115 278 2133; F: +3115 278 5006; E: j.r.vanommen@tudelft.nl

[2]Department of Chemical and Biological Engineering, University of Colorado
Boulder, CO 80309-0424, USA; alan.weimer@colorado.edu

[3]Department of Chemical Engineering, Arizona State University
Tempe, AZ 85287, USA; robert.pfeffer@asu.edu

[4]Department of Mechanical Engineering, Imperial College London
London SW7 2AZ, United Kingdom; B.van-wachem@imperial.ac.uk

ABSTRACT

The fluidization of nanoparticle agglomerates can be largely improved by using downward pointing micronozzles, creating a high-velocity jet, as experimentally shown. By discrete particle simulations – treating the agglomerates as single particles – we show that the microjet strongly reduces the amount of gas in voids.

INTRODUCTION

In recent years, the fluidization behaviour of nanoparticles has been receiving increased attention. It poses challenging scientific questions, but also has practical applications. For example, through atomic layer deposition it is possible to provide individual nanoparticles with an ultrathin coating. Weimer and co-workers demonstrated this technique for a wide variety of materials (1,2,3); recently van Ommen and co-workers showed that it is possible to carry out the process at atmospheric pressure (4). Although it sounds counterintuitive that nanoparticles could be fluidized, it is possible since they form agglomerates. Primary particles with sizes ranges from 7 to 500 nm typically form agglomerates from about 100 to 700 μm (5). These agglomerates are so dilute they are often assumed to have a fractal nature, thus making the coating of individual nanoparticles possible. Moreover, they are dynamic in nature, meaning that each agglomerate continually sheds a significant fraction of its composition, while simultaneously adding material from other agglomerates. Over the past decade, several researchers have made efforts to model the formation and fluidization of nanoparticle agglomerates (see, e.g., 6,7,8,9). Because of the large cohesive forces, fluidization aids are often needed to

obtain proper fluidization of nanoparticles. Several ways have been proposed, such as vibration, sound wave pulsation, and the use of AC electric fields (10). Recently, Quevedo et al. (11) proposed the use of microjets as an alternative. They showed that the fluidization behaviour of nanoparticle agglomerates is greatly enhanced by adding a secondary flow in the form of a high-velocity jet produced by one or more micronozzles pointing vertically downward toward the distributor. The micronozzles produced a jet with high velocity (up to near sonic velocities), breaking up large nanoagglomerates, preventing channelling, curtailing bubbling, and promoting liquid-like fluidization. In addition, they claimed that microjet-assisted nanofluidization was also found to improve solids motion and prevent powder packing in an internal, is easily scaled-up, and can mix and blend different species of nanoparticles on the nanoscale. They proposed that microjets improve the fluidization by increasing the turbulence and inducing high shear forces, which lead to agglomerate breakage. In this paper, we aim at achieving a further elucidation of the mechanisms through which a microjet enhances nanoparticle fluidization using experiments and modelling.

APPROACH

Experimental

Experiments are carried out in a glass column with a diameter of 26 mm, equipped with a porous stainless steel distributor plate and a conical freeboard section to minimize particle elutriation. A HEPA filter and water bubbler at the outlet of the freeboard ensured that no nanoparticles were released to the environment. The entire system was kept inside of a fume hood to protect operators.

The bed material consists of microfine TiO_2 (Evonik Aeroxide P-25) with a primary particle diameter 25 nm, which tend to form soft agglomerates. In all experiments except those explicitly mentioned, the powders were sieved to have a diameter between 70 and 180 μm. This enabled comparison between the jetted and unjetted systems, as unsieved powders in the unjetted bed would segregate by size and only a portion of the bed would expand. However, some experiments were completed with unsieved powders to show the magnitude of the effect of the microjet.

The bed is fluidized at atmospheric pressure and room temperature with nitrogen at superficial gas velocities ranging from 0 to 0.12 m/s. The bed was fluidized with a downward pointing tube (2mm diameter) inserted at the axis of the column; at the end of the tube a micro-nozzle has been attached with an internal diameter of 254 μm. Through the nozzle, we apply a nitrogen flow that is 30% of the base flow through the distributor.

Modelling

For the modeling of particles and fluids, different approaches and models exist, depending on the scale and region of interest. In this research, the interaction between the fluid and the particle agglomerates is of interest. Therefore, a CFD-DEM (Eulerian-Lagrangian) model was chosen. In this model, the fluid is represented as a continuous medium. Since agglomerates typically consist of billions of nanoparticles, it is not possible to model each individual nanoparticle. Instead, we model the agglomerates as spheres with a typical density and diameter

that has been found experimentally in previous studies (7,9). For simplicity, we assumed all agglomerates to have the same size, and we did not include the breakage of agglomerates. Although we realize that this is a rough approximation, we think this approach is a good first step to obtain insight in the forces that are exerted on the nanoparticle agglomerates. We intend to extend the model to include agglomerate breakage in the near future. The program that was used is MultiFlow (12). Gas-agglomerate interactions (drag force) are calculated by the Wen and Yu correlation (13). Agglomerate-agglomerate interactions are calculated using the soft-sphere approach. This type of modeling enables multiple collisions, which occur frequently in a dense fluidized bed. When agglomerates collide, they will have a reversible deformation, leading to a repulsive force between the agglomerates. The elastic deformation is approximated by allowing a small overlap, and a repulsive force model is based upon the magnitude of the overlap. The model is based upon the pioneering work of Mindlin and Deresiewicz (14) and Tsuji et al. (15). Model details and implementation can de found in Hemph et al. (16). To properly model cohesive particles, the interparticle forces are calculated by van der Waals forces according to Hamaker (17). This force is inversely proportional to the square of the interparticle distance and is characterized by the Hamaker constant which has typical values of 10^{-19} J. The agglomerate motion is calculated by integrating Newton's law of motion and the fluid is modeled by approximating the Navier-Stokes equations in a finite volume discretized framework.

Table 1: Agglomerate parameters

Property	**Value**
Model type	Lagrangian
Diameter	260 µm
Density	30 kg/m^3
Youngs modulus	1.0 GPa
Coef. of restitution	0.90
Poisson ratio	0.25
Coef. Of Friction	0.35
Number of agglom.	260,000

Table 2: System settings

Property	**Value**
Steps per collision	36
Time step hydrodynamics	$1 \cdot 10^{-4}$ s
Gravitation constant	10 m/s^2
X-dimension	$30 \cdot 10^{-3}$ m
Y-dimension	$4.0 \cdot 10^{-3}$ m
Z-dimension	$100 \cdot 10^{-3}$ m
Superficial gas velocity	$2.0 \cdot 10^{-2}$ m/s

The most important properties of the agglomerates are shown in Table 1. A value of 1.0 GPa is used for the Young modulus. The minimum fluidization velocity for these agglomerates was calculated to be 0.6 mm/s, using the Wen and Yu correlation (13). Note, however, that the Wen and Yu correlation has not been validated for particles (agglomerates) with such a low density. The properties of the walls with respect to collision are equal to the agglomerates' properties. The fluid is air at ambient conditions with a temperature of 298.15 K and a pressure of $1 \cdot 10^5$ Pa. The density of air is 1.21 kg/m^3 and the viscosity $1.52 \cdot 10^{-5}$ Pa· s.

The other simulation settings are given in Table 2. The time steps for the particle phase in the model are determined by the collisions. Each collision is calculated in 36 steps and depending on the collision properties, such as velocities and masses, a time step is calculated. The jet tip is positioned in the centre of the horizontal cross-section at $100 \cdot 10^{-3}$ m above the distributor; the jet is pointing downward. The

mesh is refined around the microjet. We carried out two different simulations: a base case with a superficial gas velocity of $2.0 \cdot 10^{-2}$ m/s and the jet turned off, and a second simulation with a superficial gas velocity of $1.4 \cdot 10^{-2}$ m/s through the distributor and a gas velocity of 18 m/s through the jet. The horizontal cross-section of the jet is 200 μm x 200 μm. The total amount of gas provided to the bed is equal for the two cases.

RESULTS AND DISCUSSION

Experiments

Before carrying out the micro-jet experiments, we have investigated the effect of isopropanol as a fluidization aid on the fluidization of nanopowders and heating and sieving as pre-processing techniques. Isopropanol is hypothesized to suppress the electrostatic forces. It also is useful in hydrating the system for de-aeration tests, so it was important to see the effect. This was completed by a bubbler system, where nitrogen, the fluidization gas, would flow through isopropanol, loading the nitrogen with isopropanol solely through the vapour pressure of the isopropanol. Subsequently, the bed heights of beds fluidized would be recorded with and without isopropanol. Bed collapse experiments were also carried out to determine if the isopropanol affected the distribution of gasses between the dense and bubble phases. However, the effect of adding isopropanol is apparent from bed collapse tests (not shown here): isopropanol leads to a slower de-aeration of the bed. Isopropanol is hypothesized to suppress the electrostatic forces between particles, but not to contribute to liquid bridging as long as it is in the vapour form. This effect would allow almost all of the nanoagglomerates to participate in the fluidization (rather than sticking to the wall or distributor), and lead to smaller bubbles, since powders would not aggregate due to electrostatics.

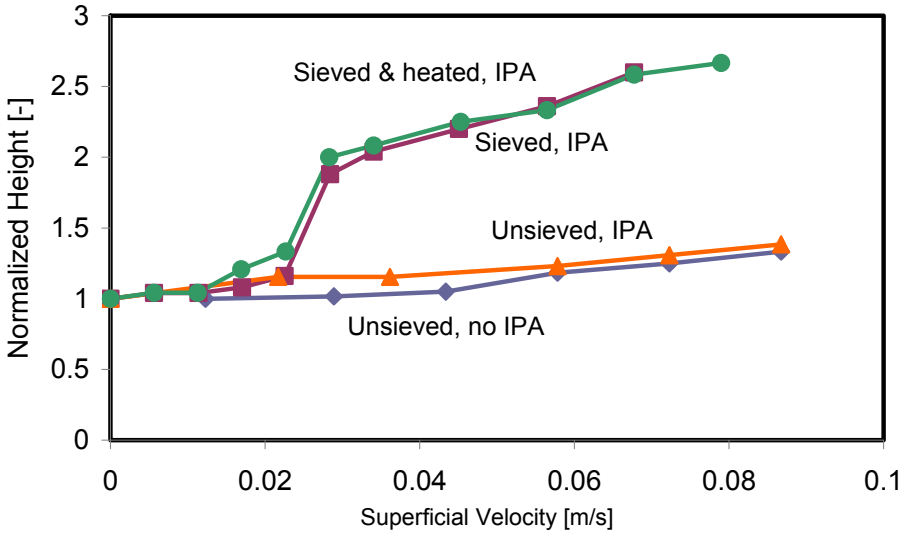

Figure 1. The effect of sieving, heating, and adding isopropanol (IPA) on the normalized bed height for the case without a microjet.

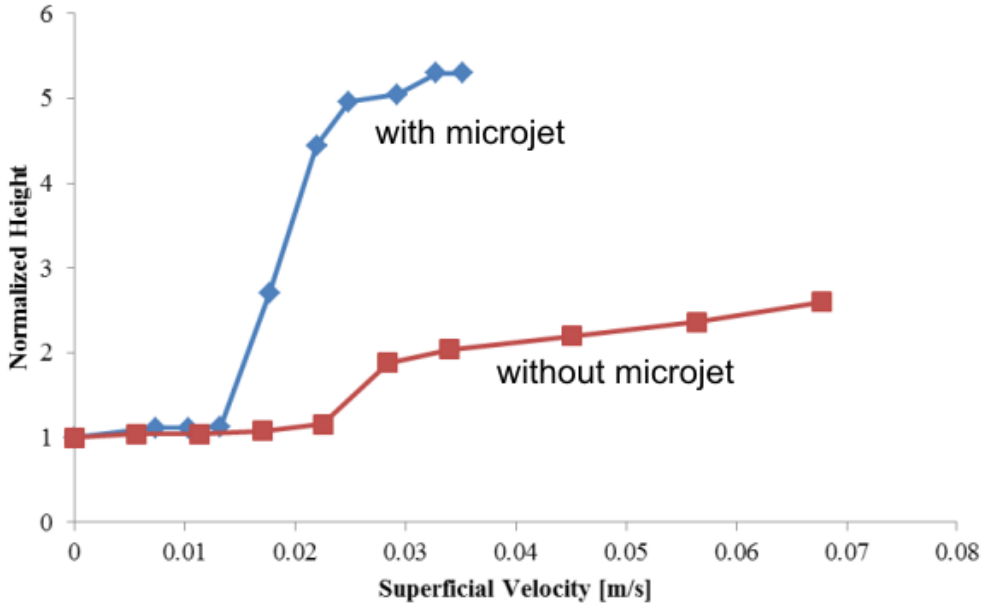

Figure 2. The powder in the bottom of the bed before and after processing with the microjet.

Figure 2 shows the stark contrast in the unjetted and jetted beds, as indicated by bed height. The jet (internal diameter 254 μm) was operated at 30% of the base flow. For the case without the jet we found a minimum fluidization velocity of 3.2 cm/s; the jet reduced the minimum fluidization velocity to 2.0 cm/s. This implies that less gas is required to fluidize the bed with a higher void fraction. Another important aspect is the amount of gas that is in the bubble and dense phases. The goal is to minimize the amount of gas in the bubble phase, especially if the fluidization gas is a reactant. Measurements of the percentages in each phase can be done using bed collapse test. In case of the jetted bed (both with sieved and unsieved material), we found an even slower bed collapse that for normal fluidization with isopropanol added. The bed collapse data indicates that the fraction of gas in the dense phase increases from 0.55 (no jet, no isopropanol) and 0.75 (no jet, with isopropanol) to

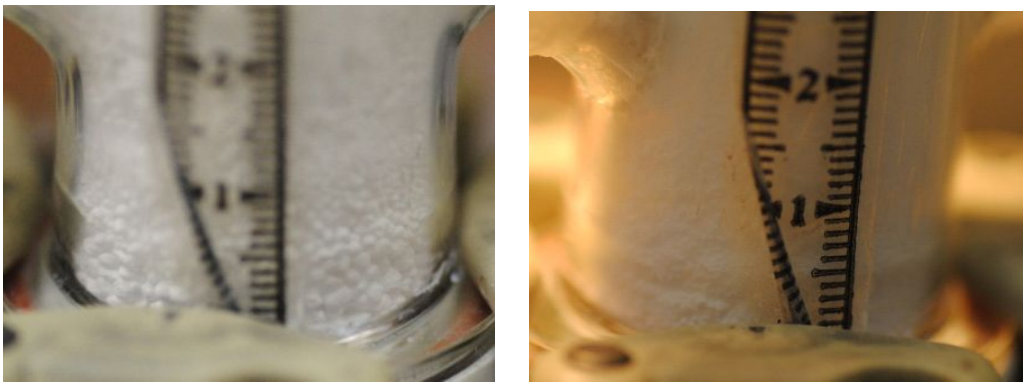

(a) **(b)**

Figure 3. The powder in the bottom of the bed (a) before and (b) after processing with the microjet. While in (a) agglomerates are clearly visible, no agglomerates can be seen in (b).

0.85-0.90 with the jet turned on and isopropanol added. This is likely due to the fact that the jet breaks up the agglomerates and diminishes the stratification. This can be seen in Figure 3. In the left-hand picture, the visible, millimetre-sized aggregates can be seen congregating in the bottom of the reactor. This formation hinders fluidization by encouraging channelling. The right-hand picture was taken after the bed was fluidized for ten minutes with the microjet turned on. This picture shows a much more homogeneous bed with no visible aggregates. Our results indicate that with the microjet no prior sieving of the bed material is needed, making it an industrially advantageous technique.

Simulations

With the simulations, it is not possible to mimic the experimental set-up completely: the amounts of nanoparticles agglomerates would become too large (>>10^6) to keep the computational times within reasonable limits. Therefore, we decided to study a pseudo 2D geometry. The depth is limited (4 mm), but large enough in term of agglomerate diameters (>10 times the agglomerate diameter). For the simulations, the ratio of the microjet cross-section (200 μm x 200 μm) compared to the bed cross-section (30 mm x 4 mm) is much larger than in the experimental setup (3.3 x 10^{-4} versus 1.6 x 10^{-5}). In order to keep the volumetric flow rate through the jet in the optimum range (10-30% of the total volumetric flow rate (11)), we used a much lower jet velocity in the simulations (18 m/s). In spite of these differences between the experimental setup and the simulations, we still expect to obtain qualitative insight in the mechanisms in which the jet enhances the fluidization of nanoparticle agglomerates. The simulations have been run for a period of 1 s of real time. Although this is a very short time, it gives us a first impression of the hydrodynamics. Longer simulations are currently being carried out.

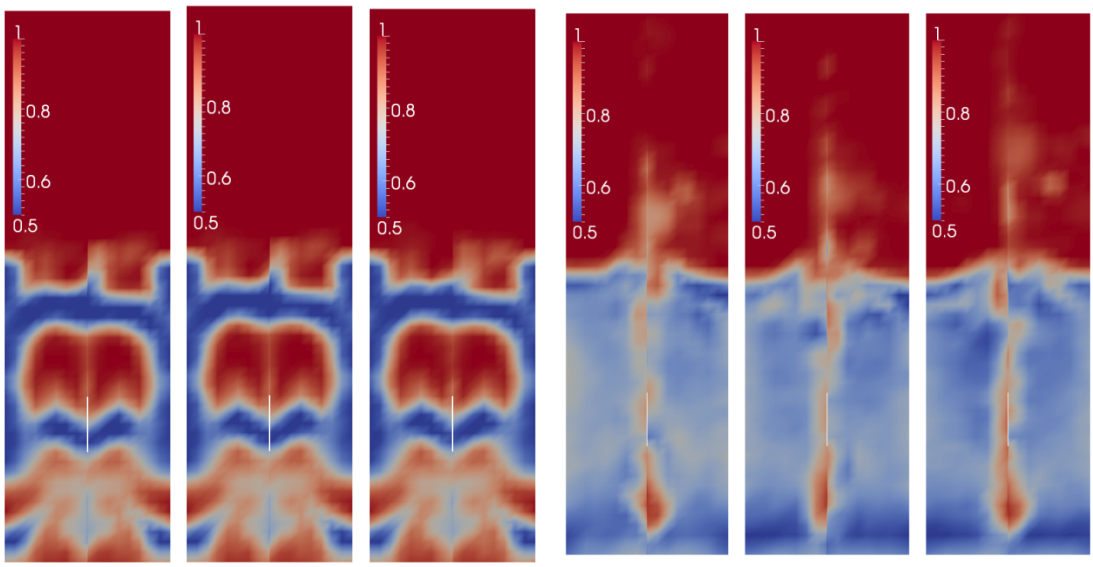

Figure 4. Snapshots of the voidage as a function of the Hamaker constant, respectively A = 0, 10^{-21} and 10^{-19} J, in the bed for (a) the jet turned off and (b) the jet turned on. The snapshots are taken 1 s after the start of the simulation.

We show the results in colour contour plots of a vertical cross section through the middle of the fluidized bed. Figure 4 shows the voidage distribution over the bed, with the jet turned off (a) and on (b). The figure clearly shows that there is a strong bubble formation in the case with the jet turned off, while the functioning jet leads to a much more homogeneous bed. Figure 4(b) does not show a large bed expansion. This means that the high jet velocity itself does not cause the large bed expansion, but rather causes the agglomerate breakage due to the action of the jet, and its impact on agglomerate-agglomerate collision frequency and force. Since these simulations assume a constant agglomerate size (i.e. agglomerate breakage is not considered), no bed height increase is observed. These results are well in line with results we reported earlier (18).

We also varied the interparticle forces during the simulations. The left-hand-side contour plots in Figs. 4(a) and (b) are the voidage distributions without interparticle forces. The middle and right-hand-side plots in Figs. 4(a) and 4(b) show the voidage for non-zero Hamaker constants, yielding low ($A=10^{-23}$ J) and normal ($A=10^{-21}$ J) magnitudes of interparticle forces. The value of the Hamaker constant seems to have little influence; even for the absence of interparticle forces (A=0 J) a very similar voidage profile is observed. The results show that the inclusion of the microjet leads to a more even distribution of the particles over the bed (i.e., absence of large voids), irrespective of the presence and magnitude of interparticle forces.

Preliminary results from both experiments and simulations (not shown in this paper) indicate that the jet just penetrates a few cm in to the bed. This means that in deeper beds than currently investigated, it is best to position the jet relatively close to the bottom, as most large agglomerates will be present in the bottom zone.

CONCLUSIONS

Experiments have shown that the fluidization behaviour of nanoparticle agglomerates is greatly enhanced by adding a secondary flow in the form of a high-velocity jet produced by a micronozzle pointing vertically downward toward the distributor. We found that the microjet increases the bed expansion and the amount of gas in the dense phase, which can be explained by a reduction in agglomerate size. Discrete particle simulations were performed using a pseudo 2D geometry, in which the agglomerates were mimicked by single particles and agglomerate breakage was not taken into account. These simulations showed that the microjet lead to a reduction of the amount of gas in voids, and a more homogeneous nature of the bed. This agrees well with the experimental findings.

NOTATION

A Hamaker constant [J]

REFERENCES

1. Hakim, L. F., Blackson, J., George, S. M., Weimer, A. W. (2005), 'Nanocoating individual silica nanoparticles by atomic layer deposition in a fluidized bed reactor', Chem. Vap. Deposition **11**, 420-425.
2. King, D.M., Johnson, S.I., Li, J., Du, X., Liang, X., Weimer, A.W. (2009), 'Atomic layer deposition of quantum-confined ZnO nanostructures', Nanotechnology **20,** 195401.
3. Liang, X., King, D.M., Li, P., George, S.M., Weimer, A.W. (2009), 'Nanocoating hybrid polymer films on large quantities of cohesive nanoparticles by molecular layer deposition ', AIChE J. **55**, 1030-1039.
4. Beetstra, R., Lafont, U., Nijenhuis, J., Kelder, E.M., van Ommen, J.R. (2009), 'Particle coating by Atomic Layer Deposition: protection of cathode material for Li-ion batteries against degradation', Chem. Vap. Deposition **15**, 227 - 233.
5. Zhu, D., Yu, Q., Dave, R.N., Pfeffer, R. (2005), 'Gas Fluidization Characteristics of Nanoparticle Agglomerates', AIChE J. **51**, 426-439.
6. Chaouki, J., Chavarie, C. Klvana, D., Pajonk, G. (1985), 'Effect of interparticle forces on the hydrodynamic behaviour of fluidized aerogels', Powder Technol. **43**, 117-125.
7. Yao, W., Guangsheng, G., Fei, W., Wu, J. (2002), 'Fluidization and agglomerate structure of SiO_2 nanoparticles', Powder Technol. **124**, 152–159.
8. Jung, J. and D. Gidaspow (2002), 'Fluidization of nano-size particles', J. Nanopart. Res. **4**, 483-497.
9. Hakim, L.F., Portman, J.L., Casper, M.D., Weimer, A.W. (2005), 'Aggregation behavior of nanoparticles in fluidized beds', Powder Technol. **160**, 149-160.
10. Lepek, D., Valverde, J.M., Pfeffer, R., Dave, R.J. (2010), 'Enhanced nanofluidization by alternating electric fields', AIChE J. **56**, 54-65.
11. Quevedo, J.A., Omosebi, A., Pfeffer, R. (2010), 'Fluidization enhancement of agglomerates of metal oxide nanopowders by microjets', AIChE J. **56**, 1456-1468.
12. van Wachem, B.G.M. (2008) MultiFlow - A fully coupled solver for multiphase flows, www.multiflow.org
13. Wen, C., Yu, Y. (1966), 'Mechanics of fluidization', Chemical engineering programming symposium **62**, 100-110.
14. Mindlin, R., Deresiewicz, H. (1953), 'Elastic spheres in contact under varying oblique forces', J. Appl. Mech. **20**, 327-344
15. Tsuji, Y., Kawaguchi, T., Tanaka, T. (1993), 'Discrete particle simulation of two-dimensional fluidized bed', Powder Technol. **77**, 79-87
16. Hemph, R., van Wachem, B., and Almstedt, A.-E. (2006), 'Distinct element modeling of hopper flows comparison and validation of models and parameters', In: Proc. Fifth World Congress on Particle Technology, Orlando, Florida.
17. Hamaker, H.C. (1937), 'The London-van der Waals attraction between spherical particles', Phyisica IV, **10**, 1-15
18. van Ommen, J.R., King, D.M., Weimer, A.W., Pfeffer, R., van Wachem (2010), 'Experiments and Modeling of Micro-jet Assisted Fluidization of Nanoparticles', in: Kim, S.D., Kang, Y., Lee, J.K., Seo, Y.C. (Eds), Proceedings of the 13th International Conference on Fluidization, pp. 479-486, Engineering Conferences International, New York.